Contents lists available at ScienceDirect

Physics and Imaging in Radiation Oncology

Short Communication

An efficient planning technique for low dose whole lung radiation therapy for covid-19 pandemic patients

Lulin Yuan [a], Siyong Kim [a,*], Jatinder Palta [a,b], Michael P. Hagan [a,b]

[a] *Department of Radiation Oncology, Virginia Commonwealth University, Richmond, VA 23219, United States*
[b] *VHA National Radiation Oncology Program Office, Richmond, VA 23249, United States*

ABSTRACT

This study aimed to establish an efficient planning technique for low dose whole lung treatment that can be implemented rapidly and safely. The treatment technique developed here relied only on chest radiograph and a simple empirical monitor unit calculation formula. The 3D dose calculation in real patient anatomy, including both nonCOVID and COVID-19 patients, which took into account tissue heterogeneity showed that the dose delivered to lungs had reasonable uniformity even with this simple and quick setup.

1. Introduction

Low dose X-ray radiation (LDIR) has been shown to have immunosuppressive effect in human. Prior to the introduction in 1939 of antibiotic therapy for pneumonia, LDIR showed promising effect for a wide spectrum of community acquired pneumonias [1]. Reviewing this experience in 2013, Calabrese and Dhawan summarized successful studies involving more than 700 patients whose pneumonias were treated with X-rays [2]. While for the past seven decades clinical evaluation of the use of ionizing radiation has centered on high-dose cancer therapies, LDIR is still being used to treat many "non-malignant disorders", such as painful arthrosis, plantar fasciitis, keloids and heterotopic ossification, etc.[3].

Many deaths from the COVID-19 pandemic were related to the lung injury caused by the inflammatory reaction of the lung [4]. Immunosuppression was suggested as possible therapy that could improve mortality for severe COVID-19 patients [5–8]. Currently, low dose radiation therapies of three fractions of 0.35–0.50 Gy up to 1 Gy in a single fraction are under investigation in clinical trials to reduce the hyperinflammatory reaction in the lung (see, e.g., [9]).

An radiation therapy treatment planning technique for such low dose whole lung treatment was introduced in this work. Due to the emergency nature of the COVID-19 pandemic and the need to initiate and deliver the LDIR in the very short time window to get possible anti-inflammatory effect [10], the goal of the study was to establish an efficient treatment technique that could be implemented rapidly and safely. A simple parallel opposed fields setup for LDIR was proposed by Kirkby and Mackenzie [6] as a proof-of-principle technique without implementation details. In this work, a treatment technique was independently presented. In addition, we proposed an monitor unit (MU) calculation method which could better account for varying patient anatomy and levels of lung consolidation, and validated it on clinical patients.

2. Materials and methods

2.1. Patient data

Twelve clinical patients (six males and six females) including two pediatric patients who had undergone cancer treatment in our institution were randomly selected in this study under an Institutional Review Board approved protocol. These patients (nonCOVID patients) had a wide range of anatomy. Among them, six patients were used to develop an MU calculation method (training patients); the other six for validation (nonCOVID validation patients). In addition, our planning method was validated on six COVID-19 patients whose computed tomography (CT) image sets were downloaded from a publicly accessible data source [10] (see the Supplementary Material for more information).

2.2. Treatment field setup

To enable rapid implementation, the treatment plan utilized

---

* Corresponding author at: Department of Radiation Oncology, Virginia Commonwealth University, 1250 E. Marshall Street, Richmond, VA 23219, United States.
  E-mail address: siyong.kim@vcuhealth.org (S. Kim).

anterior-posterior parallel opposed fields with equal weighting. A 6MV photon beam was chosen as treatment modality. The isocenter of the fields was at the mid-plane of the total lung volume along the left-right, anterior-posterior and superior-inferior directions, based on an imaging method available in the treatment room, e.g., on-board imager (OBI). The field aperture was shaped by multileaf collimator (MLC) leaves. They were drawn on the 2D radiograph to encompass the whole lung including the mediastinum with a 2 cm aperture margin. The collimator was rotated 90 degree in our system so that the MLC leaves could better conform to the outer contours of the lung. The Beam's Eye view image of the anterior treatment field for patient #7 is shown in Fig. 1(a) along with the DRR reconstructed from the CT to simulate the OBI image. Similar image for a COVID-19 patient (#6) is also shown (Fig. 1(b)). The whole planning process can be performed in the radiation therapy record and verify system while the patient is waiting.

2.3. MU calculation

The treatment planning goal was to deliver a prescription dose of 50 cGy to the mid-plane of both lungs. The dose should cover the whole lung with reasonable uniformity (approximately 15% as typically in Total Body Irradiation (TBI)). A reference point was chosen at the center of the right lung assuming both of them were similar in their dimension. MU was calculated to deliver 100% dose to the reference point. The traditional MU calculation method based on depth dose in water would not be accurate enough due to the lower density of lung tissue. The nomograph method provided in [11] to relate lung dose correction factors with patient thickness in the context of TBI cannot account for the wide variation of lung density caused by the pathophysiological changes in lung tissue seen in COVID-19 patients [12]. In this work, 3D dose calculation was performed in our clinical treatment planning system (Eclipse V13.7, Varian Medical System) using AcurosXB algorithm with inhomogeneity correction turned on. AcurosXB is an implementation of the numerical solver to the linear Boltzmann transport equation [13]. It has been shown to have less than 3% difference from Monte Carlo type of algorithm in heterogeneous medium [13,14].

It has been observed that an important symptom of COVID-19 patients is the inflammation of the lung tissue. The inflammation causes diffuse ground-glass infiltration in the lung which increases the density of the lung to a varying degree [12]. To better represent this pathologic change without 3D information, we artificially altered the lung density uniformly in the treatment planning system. Radiologically, the degree of fibrosis of the lung tissue can be quantified by consolidation, with normal lung density (assumed to be ~0.2 gm/cm^3) equivalent to zero (0) consolidation and a lung full of fluid (water) 1.0 (i.e., 100%). In this study, we assumed a linear relationship between the consolidation obtained from planar lung x-ray and the average density of the lung. Thus, we used the following formula to convert the density (in gm/cm^3) to consolidation:

$$\text{Consolidation} = 1.25 \times (\text{Density} - 0.2) \tag{1}$$

We assigned the lung tissue to a number of different densities to simulate lung consolidation at 25%, 50% and 75%, in addition to the clinical lung density from CT.

To enable rapid implementation of this treatment technique, an empirical formula was derived to calculate MUs directly from a simple measurement of patient thickness as the anterior-posterior separation at mid-sternum level and a chest radiograph to clinically assess lung consolidation. However, since this study was performed on retrospective dataset, the thickness was measured equivalently from CT images. A linear multiple regression method was used to fit a correlation between the MU and the patient body thickness and lung consolidation from six training patients (24 training cases in total after density override). The treatment planning method and the MU calculation formula were validated with the remaining six nonCOVID patients with various levels of lung density override and six COVID-19 patients. The dose at the center of the lung, as well as the maximum and mean lung dose were extracted to evaluate the dosimetric quality of the treatment technique.

3. Results

The MUs for the training patients with clinical CT lung density and altered lung densities were in the range from 24.3 to 30.4. Within the nonCOVID patients, the actual lung consolidations were in the range of −0.03 to 0.35. Both the two pediatric patients had higher lung consolidation than all the adult patients. The lung consolidation within the COVID-19 patients was from 0.0 to 0.19.

The formula to calculate MU per field is given below in terms of MU per cGy of prescription dose so it can be applied to different prescription dose levels:

$$\text{MU/cGy} = 0.426 + 0.0036 \times \text{Body}_{\text{Thickness}}(\text{incm}) + 0.086 \times \text{Consolidation} \tag{2}$$

The regression coefficient of determination was 0.83 and the largest relative MU error was 4.5% with this formula. The MU, body thickness and lung consolidation for these plans are shown as scatter plots on Fig. 2.

Among the nonCOVID validation patients, the maximum deviation for the mid-lung dose was 3% (range: 98–103%) and the range of maximum and mean lung dose were from 106% to 113% and from 94%
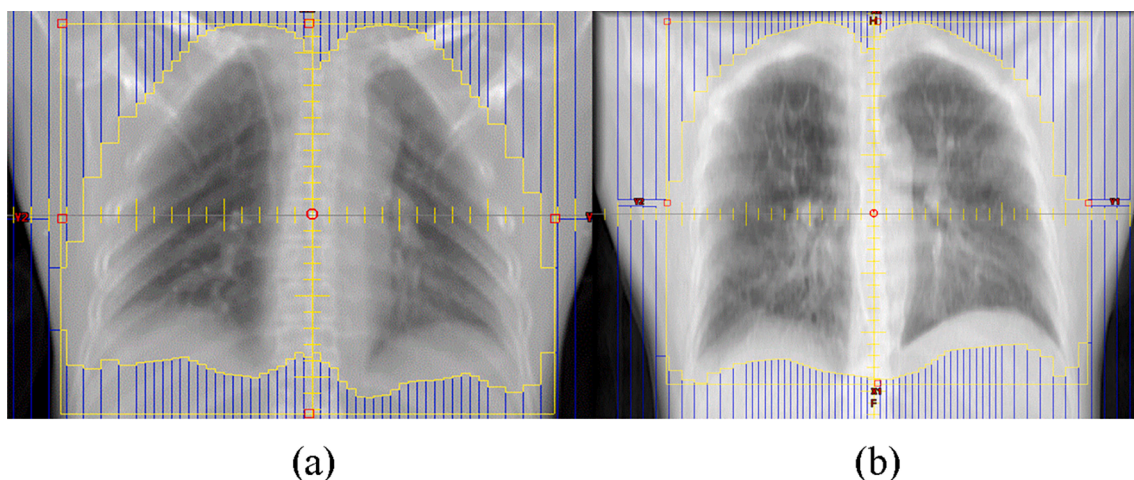

Fig. 1. (a) Beam's Eye view image of the AP treatment field for patient#7 along with the DRR reconstructed from the CT image set to simulate the x-ray radiograph. Blue lines indicate MLC positions. Each division on the field graticule represents one 1 cm. (b) The AP treatment field and DRR for COVID-19 patient #6.
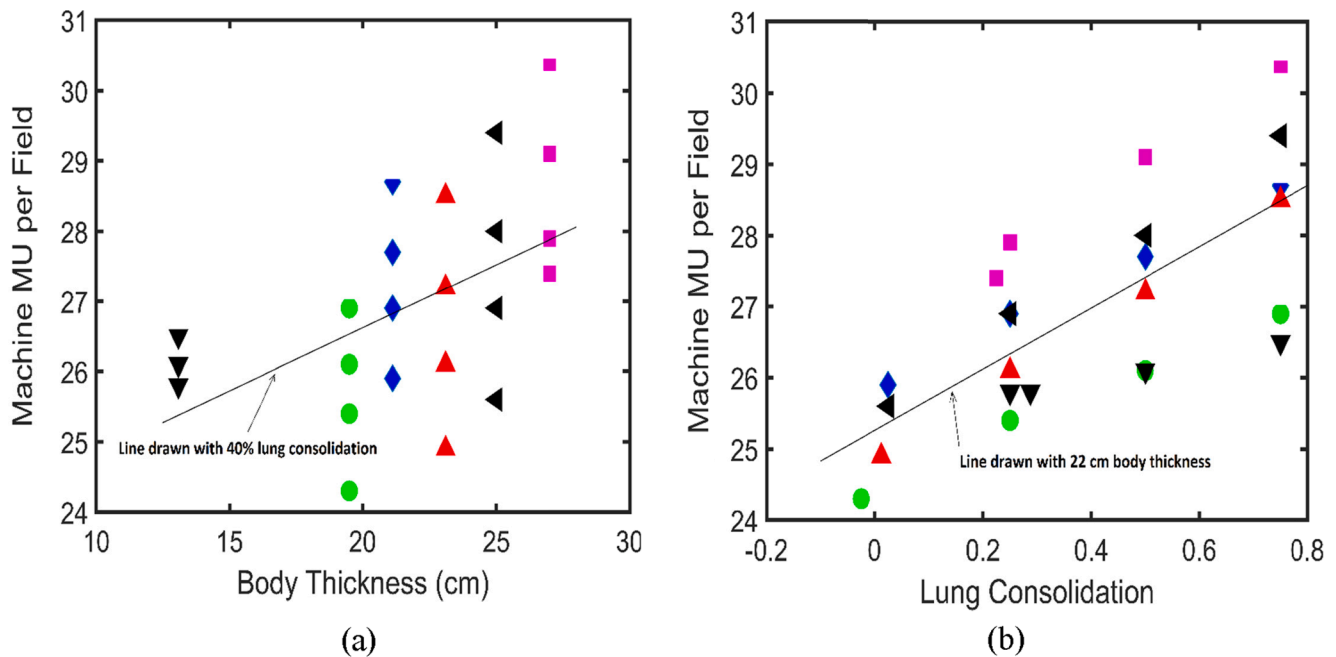
Fig. 2. (a) The correlation between machine MUs and patient body thickness for the six training patients with different levels of lung density override (actual patient lung consolidation, 25%, 50% and 75%) shown as scatter plot. Each marker represents one plan. The different types of markers represent different patients. The line drawn on the plot shows the trend of the correlation. It is plotted according to Eq.2 with a constant lung consolidation of 40%. (b) Scatter plot of the MUs and lung consolidations. The line represents the correlations with a constant body thickness of 22 cm. The actual body thickness for the patients are: 21.1, 19.5, 27.0, 25.0, 23.1 and 13.9 (all in cm), respectively.

to 103%, respectively. The largest deviation in mean dose (−6%) was from a validation patient (#11) with thick breast tissue (~7 cm) and actual CT lung consolidation of 0.19. Among the COVID-19 patients, the range for the mid-lung dose was from 100% to 105%, maximum lung dose: from 108% to 114% and mean lung dose: from 97% to 100%, respectively. The detailed dose/volume metrics are shown in Supplementary Table S1 for the nonCOVID validation patients and Table S2 for the COVID-19 patients, respectively. The isodose distributions for the COVID-19 patients are shown on their CT images in Supplementary Fig. S1.

4. Discussion

The goal of this study was to find an efficient treatment technique for low dose whole lung treatment so it could be implemented rapidly and safely. The treatment technique relied only on chest radiograph obtained using a portable X-ray unit or OBI and a simple empirical MU calculation formula. Dose calculation in real patient anatomy showed that acceptable dosimetric quality could be achieved by this efficient technique.

For a patient with very large lung volume, the Field-of-View of the imaging system may not be large enough to capture the whole lung in a single image. In such cases, it may be helpful to move the imager closer to the patient, and move both the patient & imager towards the source or by combining several partial images together. Another issue with lung radiograph is that a single radiograph may miss-represent the diaphragm position due to its respiratory motion. However, study has shown that the superior-inferior motion of lower lung lobe is mostly within approximately 2 cm [15]. Thus additional 2 cm margin could be enough to encompass the motion in most cases. In addition, multiple images can be taken and the largest can be chosen for planning.

For the sake of workflow efficiency, we have made two approximations. First, we utilized a linear regression method to fit the MU calculation formula. However, as can be seen from Fig. 2, a nonlinear function can possibly better describe its dependence on body thickness, especially for patients with very small lung volume. Secondly, the thicknesses of

the breast and chest wall were not taken into account in the MU calculation. We can see that these are reasonable assumptions based on the small variation in the actual mid-lung dose among the validation patients.

In this work, the ArucosXB algorithm was used and the lung consolidation was considered to improve dose calculation accuracy inside lung. AcurosXB has been shown to be more accurate than the convolution-superposition type of algorithms, especially in the low density lung tissues and the lung soft tissue interface [16,17]. However, we realized that the determination of lung consolidation level from either chest X-ray or an OBI image may have large uncertainty. Another limitation with the 2D projective imaging is that it lacks information on the 3D distribution of lung density. Thus we made the approximation that the consolidation is uniform over the whole lung. The approximation is based on the observation from Eq. (2) that the delivered dose is not very sensitive to the variation in lung consolidation: a 10% change in consolidation results in about 2% deviation on mid-lung dose. Similar observation has been made in a previous study which concluded that the dosimetric impact of the CT number variation is limited in low density medium [18]. This approximation is also supported by the radiographic studies of COVID-19 patients that show extensive diffuse ground-glass opacities with consolidation in the lungs of later stage patients [12].

It should be pointed out that the MU calculations in Eq. (2) are associated with the output calibration condition for the linac in our clinic, which is described in detail in the Supplementary Material. Therefore, readers should validate them on their own machines and under their own setup conditions, and establish the equivalent formula for these conditions [19,20]. For instance, in the case of different calibration condition for reference dosimetry, the derived MU will have to be corrected using the well-established correlation between two different setup conditions for output calibration [14].

In conclusion, an efficient planning technique for low dose whole lung treatment was presented in this work. 3D dose calculation in real patient anatomy, including both nonCOVID and COVID-19 patients, showed that the dose delivered to the lungs had reasonable uniformity even with this simple and quick setup.

Declaration of Competing Interest

The authors declare that they have no known competing financial interests or personal relationships that could have appeared to influence the work reported in this paper.

Appendix A. Supplementary data

Supplementary data to this article can be found online at https://doi.org/10.1016/j.phro.2020.10.004.

References

[1] Quimby A, Quimby W. Unresolved pneumonia: successful treatment by roentgen ray. N Y Med J 1916;103:681–3.

[2] Calabrese EJ, Dhawan G. How radiotherapy was historically used to treat pneumonia: could it be useful today? Yale J Biol Med 2013;86:555–70.

[3] Seegenschmiedt MH, Micke O, Muecke R. Radiotherapy for non-malignant disorders: state of the art and update of the evidence-based practice guidelines. Br J of Radiol 2015;88:20150080.

[4] Conti P, Gallenga CE, Tetè G, Caraffa A, Ronconi G, Younes A, et al. How to reduce the likelihood of coronavirus-19 (CoV-19 or SARS-CoV-2) infection and lung inflammation mediated by IL-1. J Biol Regul Homeost Agents 2020;34.

[5] Mehta P, McAuley DF, Brown M, Sanchez E, Tattersall RS, Manson JJ. COVID-19: consider cytokine storm syndromes and immunosuppression. Lancet 2020;395 (10229):1033–4.

[6] Kirkby C, Mackenzie M. Is low dose radiation therapy a potential treatment for COVID-19 pneumonia? Radiother Oncol 2020;147:221.

[7] Venkatraman P, Sahay JJ, Maidili T, Rajan R, Pooja S. Breakthrough of COVID-19 using radiotherapy treatment modalities. Radiother Oncol 2020;148:225–6.

[8] Dhawan G, Kapoor R, Dhawan R, Singh R, Monga B, Giordano J, et al. Low dose radiation therapy as a potential life saving treatment for COVID-19-induced acute respiratory distress syndrome (ARDS). Radiother Oncol 2020;147:212–6.

[9] Emory University and National Cancer Institute. Radiation Eliminates Storming Cytokines and Unchecked Edema as a 1-Day Treatment for COVID-19. https://ClinicalTrials.gov/show/NCT04366791; 2020 [accessed 12 Aug 2020].

[10] Bell DJ, et al. COVID-19. https://radiopaedia.org/articles/covid-19-4?lang=us; 2020 [accessed 3 Aug 2020].

[11] Dyk JV, Galvin JM, Glasgow GP, Podgorsak EB. AAPM Report No. 17: The Physical Aspects of Total and Half Body Photon Irradiation. American Association of Physicists in Medicine; 1986.

[12] Shi H, Han X, Jiang N, Cao Y, Alwalid O, Gu J, et al. Radiological findings from 81 patients with COVID-19 pneumonia in Wuhan, China: a descriptive study. Lancet Infect Dis 2020;20:425–34.

[13] Gifford KA, Horton JL, Wareing TA, Failla G, Mourtada F. Comparison of a finite-element multigroup discrete-ordinates code with Monte Carlo for radiotherapy calculations. Phys Med Biol 2006;51:2253–65.

[14] Khan FM. The physics of radiation therapy. 3rd ed. Baltimore: Lippincott Williams & Wilkins; 2003.

[15] Keall PJ, Mageras GS, Balter JM, Emery RS, Forster KM, Jiang SB, et al. The management of respiratory motion in radiation oncology report of AAPM Task Group 76a). Med Phys 2006;33:3874–900.

[16] Yan C, Combine AG, Bednarz G, Lalonde RJ, Hu B, Dickens K, et al. Clinical implementation and evaluation of the Acuros dose calculation algorithm. J Appl Clin Med Phys 2017;18:195–209.

[17] Han T, Followill D, Mikell J, Repchak R, Molineu A, Howell R, et al. Dosimetric impact of Acuros XB deterministic radiation transport algorithm for heterogeneous dose calculation in lung cancer. Med Phys 2013;40:051710.

[18] Das IJ, Cheng C-W, Cao M, Johnstone PAS. Computed tomography imaging parameters for inhomogeneity correction in radiation treatment planning. J Med Phys 2016;41:3–11.

[19] TRS 398: Absorbed dose determination in external beam radiotherapy: an international code of practice for dosimetry based on standards of absorbed dose to water. Vienna: International Atomic Energy Agency; 2001.

[20] Almond PR, Biggs PJ, Coursey BM, Hanson WF, Huq MS, Nath R, et al. AAPM's TG-51 protocol for clinical reference dosimetry of high-energy photon and electron beams. Med Phys 1999;26:1847–70.